FEBS Letters 569 (2004) 54–58 FEBS 28501

Kinesin heads fused to hinge-free myosin tails drive efficient motility

Verena Eickel[a], Douglas Drummond[a], Nick Carter[a], Andrew Lockhart[a,b], John Kendrick Jones[b], Robert Cross[a,*]

[a] *Molecular Motors Group, Marie Curie Research Institute, The Chart, Oxted, Surrey RH8 0TL, UK*
[b] *MRC Laboratory of Molecular Biology, Hills Road, Cambridge CB2 2QH, UK*

Received 17 February 2004; revised 17 May 2004; accepted 17 May 2004

Available online 7 June 2004

Edited by Amy McGough

Abstract The rat kinesin motor domain was fused at residues 433, 411, 376 or 367, respectively, to the C-terminal 1185, 1187, 1197 or 1185 residues of the brush border myosin tail. In motility assays, K433myt and K411myt, which preserve the head-proximal kinesin hinge, and K367myt, which deletes it, drove rapid microtubule sliding ($\sim$0.6 μm s^{-1}) that was optimal when the head-pairs were spaced apart by adding 1:1 headless myosin tails. K376myt, which partially deletes the head-proximal hinge, showed poor motility in sliding assays but wild type processivity, velocity and stall force in single molecule optical trapping. Accordingly, the head-proximal kinesin hinge is functionally dispensable.

Keywords: Kinesin; Processivity; Optical trap; Myosin tail; Myosin filament; Myosin self-assembly

1. Introduction

The classical kinesin (KHC, kif5b, kinesin-1) has twin heavy chains, of which the N-terminal $\sim$340 residues form globular head domains. The remaining $\sim$600 residues of each chain wrap together into a two-chain α helical coiled coil, interrupted at 3 positions by substantial stretches of pro and gly-rich sequence, assigned as hinges in the structure [1]. The heads contain the microtubule binding and ATPase sites, and are attached to the tails via 13 residue neck linker domains [2,3], recently proposed to reversibly dock and undock to the main part of the heads as the kinesin molecule steps along the microtubule [4].

Single, two-headed molecules of kinesin translocate using a head-over-head ''walking'' action along microtubules [5], moving 8 nm [6,7] and consuming about 1 ATP per physical step [8–10]. The mechanism by which the two walking heads coordinate their mechanical actions is an important biological problem that is receiving a great deal of attention. No less interesting, however, is the mechanism by which multiple molecules of kinesin on a surface can collaborate so as to drive smooth motility of overlying microtubules. This multimolecule mode of kinesin has been known since the early days of kinesin science [11], but its mechanisms have received much less attention than those of the single molecule mode. Yet the multimolecule mode may be the more biologically relevant – certainly in the case of non-processive kinesin family members, such as those involved in mitotic spindle dynamics, substantial forces are developed as a result of coordinated molecular teamwork [12].

Concerning the molecular mechanism of teamwork, one would like for example to ask, how densely packed is an ideal kinesin array? Does molecular orientation affect teamwork? Are there mechanical elements of the molecule that are specifically concerned with teamwork, or is effective teamwork a consequence of the same coordination mechanisms that drive single molecule walking? To begin to probe mechanisms of intermolecular collaboration in kinesin teams, and in particular the requirement for the head-proximal hinge (Fig. 1), we wanted to engineer a small number of kinesin molecules into an oriented ensemble. We describe here characterisation of the protein products of a number of constructs that fuse a self-assembly domain, the tail of brush border myosin II, into the head-proximal hinge of the kinesin tail at various points. The series deletes progressively through the hinge, potentially affecting the mobility of the kinesin heads. We find, however, that even our most substantial truncation (K367myt), which effectively replaces the kinesin tail with a continuous, hinge-free coiled coil, shows essentially wild type behaviour in single molecule optical trapping assays, and in multimolecule surface sliding assays also, provided that a certain minimum spacing is introduced between the kinesin heads.

2. Materials and methods

Fusion constructs were engineered by PCR, restriction digestion and ligation from a full length rat kinesin (Scott Brady) and a chicken brush border myoII tail (pIN II A3) [15]. The rat kinesin motor domains 1–433, 1–411, 1–376 or 1–367 were fused, respectively, to the C-terminal 1185, 1187, 1197 or 1185 residues of the brush border myosin tail. The constructs were inserted into pET17b modified to attach a tag GSSGGSSGGSSGLAAAHHHHHH directly to the C-terminus of the myosin tail. Following expression [13] bacteria were lysed into 50 mM Na phosphate pH 7.5, 5 mM $MgCl_2$, 10 mM 2-mercaptoethanol, 600 mM NaCl plus protease inhibitor cocktail (Roche, 1 tablet per 50 ml). The extract was treated with lysozyme and DNAase [13], centrifuged at 33 600 × *g* for 30 min at 4 °C, diluted fivefold with 50 mM Na phosphate, pH 6.5, 5 mM $MgCl_2$, 10 mM 2-mercaptoethanol, 20 mM NaCl, 0.25 mM PMSF, 1 mM EGTA and re-centrifuged at 33 600 × *g* for 30 min at 4 °C. The pellet of assembled material was re-dissolved in lysis buffer, centrifuged at 13 000 × *g* for 15 min at 4 °C and applied to a Superose 6 column equilibrated with lysis buffer and run at 0.2 ml min^{-1}. Peak fractions were supplemented with 20% glycerol and flash-frozen in liquid N_2. Purity of the full-length protein was >60%; contaminants were chiefly proteolytic fragments of the myosin tail that carried the hexahistidine tag. For expressed myosin tail only, the ex-

* Corresponding author. Fax: +44-1883-714-375.
E-mail address: r.cross@mcri.ac.uk (R. Cross).

0014-5793/$22.00
doi:10.1016/j.febslet.2004.05.050

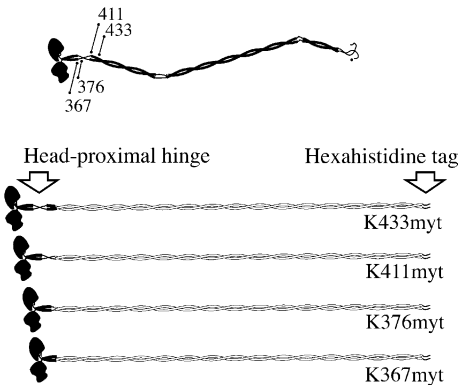

Fig. 1. Different fusion constructs. (Top) Organisation of the kinesin heavy chain. (Beneath) Fusion constructs. The kinesin component is shaded and the myosin component is unshaded. The mutants progressively delete through the tail hinge 1 and contain no other tail hinges.

tract was boiled, centrifuged at 33 600 × *g* for 30 min at 4 °C, assembled by dilution, sedimented, redissolved, clarified, supplemented with glycerol and frozen. Purity of the full-length protein was >80%. Tubulin was prepared as in [13]; protein concentrations were determined spectrophotometrically using calculated extinctions. Motility assays and optical trapping were as in [14].

3. Results

3.1. Self-assembly of kinesin head myosin tail fusions

A schematic of the constructs is shown in Fig. 1. At low ionic strength, all the fusions assembled into short filaments, clearly visible in video enhanced DIC light microscopy (Fig. 2D). Negative stain electron microscopy (Fig. 2A and B) confirmed a side-polar molecular packing arrangement, in which the filaments clamped their constituent molecules so as to align the tails almost parallel to the long axis of the filaments. The filaments resembled those formed from isolated (headless) tails of brush border myosin II [15]. The cartoon (Fig. 2C) indicates a possible packing arrangement, with opposite sides of the filament having opposite polarity and a 14.3 nm intermolecular stagger corresponding to that worked out earlier for smooth muscle myosin [16]. The visible protrusions (white arrows) may correspond to kinesin head-pairs. The size of these filaments and the number of filaments per unit volume

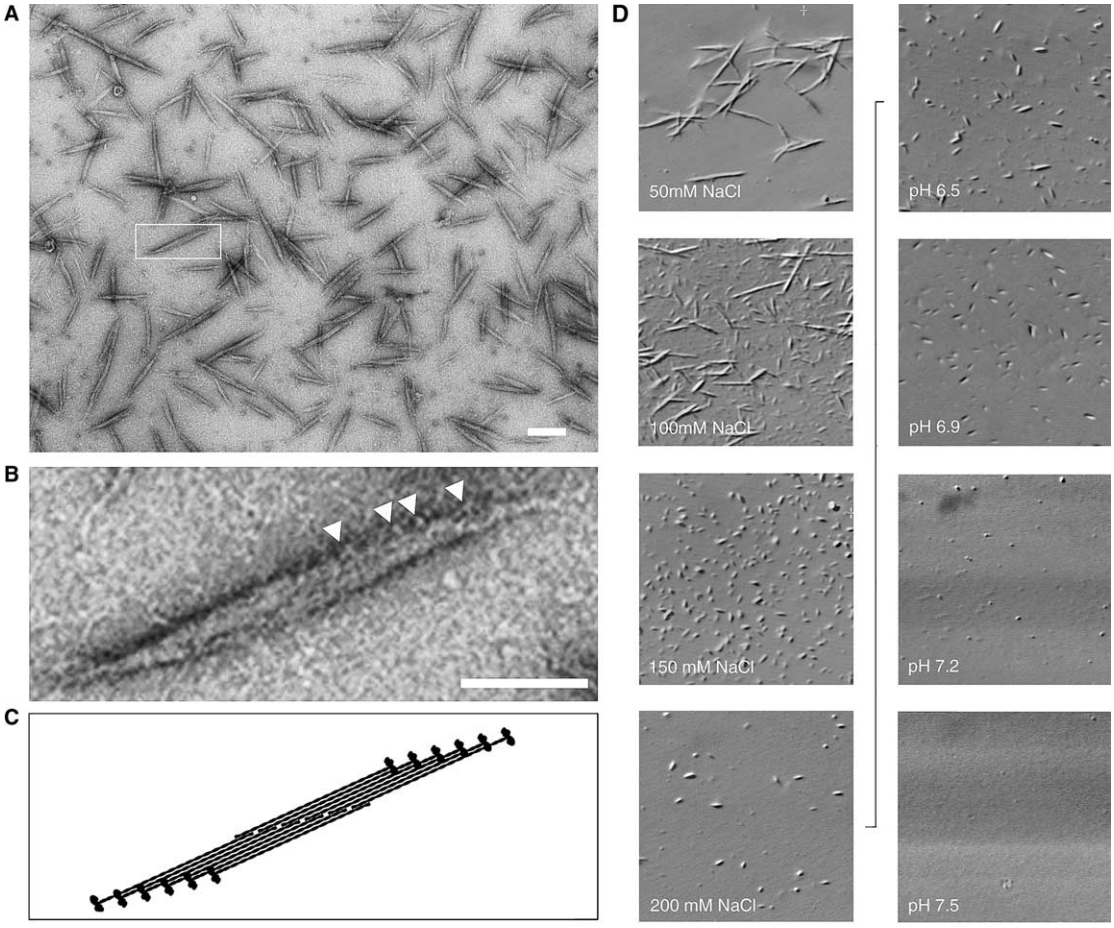

Fig. 2. Imaging of K-myt filaments. Filaments were assembled by dialysis of K433myt against 50 mM Na phosphate, 5 mM $MgCl_2$, 1 mM DTT, pH 6.5, plus various concentrations of NaCl, or against 200 mM NaCl, 5 mM $MgCl_2$, and 1 mM DTT, adjusted to various pHs. (A) Negative stain EM imaging of K433myt filaments in 175 mM NaCl and 10 mM Pi, pH 7.0. Scale bar is 0.2 μm. (B) Zoom view of the boxed region in (A). Scale bar is 0.1 μm. Protrusions that may correspond to kinesin head-pairs are apparent (white chevrons). (C) Cartoon showing a possible molecular packing arrangement. (D) Video enhanced DIC optical microscope images showing progressive decrease in filament size and number concentration with increasing NaCl concentration (left column) and increasing pH (right column, salt concentration fixed at 200 mM). Field = 25 μm.

were strongly dependent on protein concentration, pH, and ionic strength (Fig. 2D).

3.2. Randomly oriented K-myt motors drive rapid microtubule sliding

In 0.6 M NaCl buffer, the various fusions were depolymerised. When applied to glass coverslips under these conditions, all four constructs adhered well and formed a smooth lawn which drove microtubule sliding. Large data sets were collected so as to detect slight effects. K433myt and K411myt, which both contain hinge 1, and K367myt, which completely deletes hinge 1, drove microtubule sliding at identical rates (Fig. 3). K376myt substantially but incompletely deletes hinge 1 and was aberrant: microtubules adhered poorly to K376myt surfaces and the motility of those that did stick was substantially reduced.

3.3. Including headless tails as spacers identifies an optimal intermotor spacing

The myosin fusion constructs afford the possibility to change the average intermolecular spacing on the surface in a controlled way, by mixing headless myosin tails with the motor in various proportions.

Figs. 4A and 4B show that even under high salt conditions, when any self-assembly is blocked, such a titration produces a peak at around a 1:1 ratio of headless myt to K-myt. As the proportion of added myt increases, there is at first an increase in sliding velocity, but then adding still more tails decreases sliding velocity.

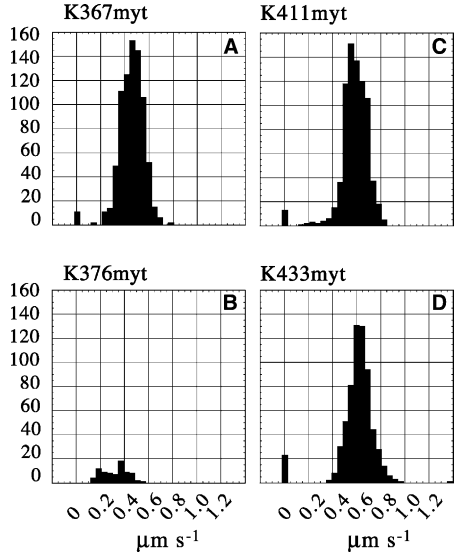

Fig. 3. Microtubule surface sliding velocities for the different fusion constructs. Distributions of microtubule velocities in surface sliding assays using different kinesin–myosin fusion proteins. Surfaces were prepared by irrigating with 10 μM motor in a high salt solution (50 mM Na phosphate, pH 7.3, 500 mM NaCl, 5 mM $MgCl_2$, and 1 mM DTT) and then rinsed with high salt buffer. Microtubules were then added in BRB80 + 2 mM ATP. All the microtubules in each field examined were tracked. The *Y*-axis is the number of instances of a particular instantaneous velocity (one time lapsed video frame to the next) across multiple fields of multiple flow-cells. (A) The mean velocity of K367myt was 0.47 $\mu m\,s^{-1} \pm 0.09$ S.D. (B) Only a few microtubules attached to the K376myt surface and many of those that did attach did not show motility. Those that moved did so at a mean velocity of 0.32 $\mu m\,s^{-1} \pm 0.10$ S.D. (C) The mean velocity of K411myt was 0.60 $\mu m\,s^{-1} \pm 0.07$ S.D. (D) The mean velocity of K433myt was 0.62 $\mu m\,s^{-1} \pm 0.08$ S.D.

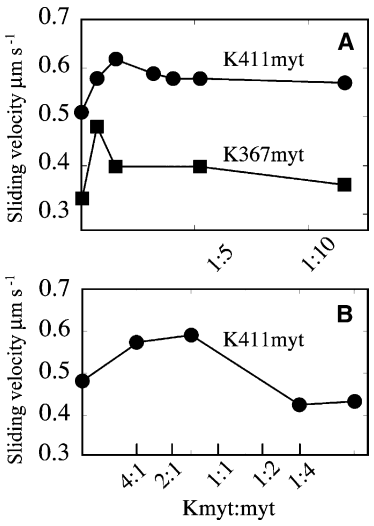

Fig. 4. Headless myosin tails as spacers. Surfaces were prepared by application of mixtures of K411myt and myt (20 μM total concentration) in 600 mM NaCl, 50 mM Na phosphate, pH 7.5, 5 mM $MgCl_2$, 1 mM DTT, and post-rinsing with this same buffer before adding microtubules in BRB80 plus 2 mM ATP. The *X*-axis plots the proportion of K-myt:myt. (A) A peak of sliding velocity at around 1:1 K-myt:myt is apparent. (B) A subsequent experiment confirming the peak of sliding velocity at about 1:1 myt:K411myt.

3.4. Microtubule sliding over K-myt filaments attached to surfaces

Microtubules slid in straight lines over K-myt filaments attached to the glass coverslip, showing no tendency to align on the oriented teams of motors in the filaments, but rather moving smoothly over both these and the randomly oriented molecules originally in equilibrium with the filaments and now lying in the background. K-myt filaments bound tightly to the glass coverslip and were never seen to detach from the glass and move along microtubules. As with the surfaces laid down under high-salt conditions, supplementing the assembly mixtures with 1:1 headless tails produced optimal sliding velocity (data not shown). Smooth microtubule sliding over these mixed surfaces of filaments and dispersed molecules might mean (a) that self-assembly and the attendant clamping of molecular orientation in the filaments have no effect on kinesin head function, or (b) that kinesin heads in the K-myt filaments were completely non-functional, and that the observed motility on filament preparations is in fact driven by randomly adsorbed disperse molecules in the background. Because microtubules slid at the same velocity over surfaces coated with filament preparations and surfaces coated with dispersed motor, we must leave open the formal possibility that kinesin heads in filaments are unable to interact with microtubules. The only thing we can definitively rule out is that self-assembly *partially* inhibits the K-myt molecules in the filaments, because we would have detected this as a slowing down of microtubules that slid over the immobilised filaments.

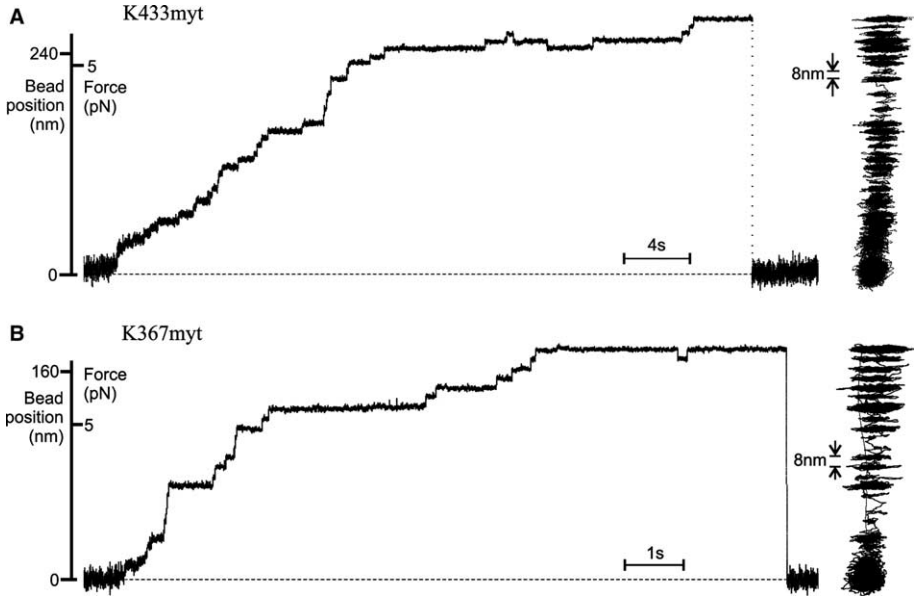

Fig. 5. Records from single molecule infrared optical trap assays. Representative infrared optical trapping record obtained from a single molecule of (A) K433myt hinge *plus*, 800 nm bead diameter, trap stiffness 0.022 pN/nm, data rate 5 kHz, 5 ms boxcar filtered, 2 μM ATP or (B) K367myt hinge *minus*, 440 nm bead, trap stiffness 0.042 pN/nm, 100 kHz sample rate, 3 ms boxcar, 10 μM ATP. Vertical deflection represents excursion away from the trap centre (dotted line) and along the microtubule axis. Both constructs demonstrated 6–8 pN stall forces. To the right of each record, the data are replotted in *XY*, showing both on-axis and off-axis bead movement. 8 nm steps are clearly visible. Conditions: beads were prepared and traces recorded in BRB-80 (80 mM K-PIPES, 1 mM $MgCl_2$, and 1 mM EGTA pH 6.9) with 5 mM DTT and 0.2 mg/ml casein block. Motor was adsorbed to beads in the presence of 500 mM NaCl to ensure single molecule adsorption. Records are of single molecules based on the quantised 6–8 pN stall force routinely obtained. All records were made in the presence of a glucose, glucose oxidase and catalase oxygen scavenging system.

3.5. *Hinge-minus and hinge-plus constructs are indistinguishable in the optical trap*

The surface sliding data suggest that any flexibility provided by the head-proximal hinge 1 is unnecessary for efficient function of kinesin teams. It is not clear, however, to what extent multiple kinesins on a surface retain the walking action (mechanical processivity) that allows single molecules to progress along microtubules for up to several hundred steps. Furthermore, surface sliding assays do not return information about the influence of external force on the stepping action of the motor. To assay single molecule performance under an external load, we used a custom built infrared optical trap [14]. Fig. 5 shows that both the hinge-plus mutant K433myt and the hinge-minus mutant K367myt were processive, that both progressed in 8nm steps and that both stalled at 6–8 pN of retroactive optical force. K376myt showed similar behaviour (data not known).

4. Discussion

Assays that measure the velocity of microtubule sliding over surfaces coated with kinesin are routinely used in kinesin research, yet the mechanisms by which the surface-bound motors are able to join forces remain mysterious. Depending on the detailed mechanism of stepping, the torsional and flexural rigidity of the mounting on which the kinesin heads are displayed towards the microtubule might substantially affect performance, both of single molecules and of teams. Current models posit diffusional searching by tethered heads for a binding site on the microtubule, followed by a transition to tight binding, one or more directional conformational changes, and subsequent detachment [17]. Rate constants for all of these processes could be affected by the torsional and flexural rigidity of the proximal part of the tail, and indeed existing data suggest that progressive truncation of the tail does progressively slow down the sliding assay [18,19].

Our data on mixtures of head-containing (K-myt) constructs and headless myosin tails (myt) suggest that performance of a close packed lawn of the motor may be limited by mutual interference effects, and that these can be relieved by introducing an inert spacing molecule. The reduction of sliding velocity at high concentrations of added tails (and sparser kinesin heads) suggests that some molecular friction occurs between the microtubules and the myosin tails.

Our data further indicate that K367myt, which mounts the kinesin heads on a hinge-free tail, is fully functional in single molecule processivity, and drives microtubule sliding in surface assays at a rate indistinguishable from wild type. We can accordingly rule out that the head-proximal hinge 1 is necessary for processive stepping of kinesin. This conclusion potentially conflicts with that of Grummt et al. [20], who described the inhibitory effect of hinge 1 deletion from a fungal kinesin on the rate of microtubule surface sliding. The initial Grummt et al. experiments were aimed also at creating a continuous, hinge-free coiled-coil tail. The main differences between their experiments and ours are (a) that they were working with a fungal kinesin, nkin, and (b) that they deleted a section corresponding to the hinge 1, thereby bringing the C-terminal boundary of the hinge 1 into apposition with the dimerisation domain. The behaviour they reported for this mutant is similar to that of our K376myt, which resembles their mutant in that it

retains a few residues of the head-proximal hinge. The important point is that in our hands the motility defect of K376myt appears specific for the surface assay; K376myt works well in single molecule processivity assays.

Aside from demonstrating that the head-proximal hinge 1 is dispensable for sliding function, the current work also offers a proof of principle that self-assembly can be used to orient kinesin heads and distribute them on a known intermolecular net, with the potential to investigate collaboration mechanisms linking members of the resulting molecular ensembles. We hope now to develop this approach to allow dissection of the mechanisms of intermolecular collaboration in other kinesin arrays. In particular, we are hopeful that the approach can be pursued to study kinesin teams in the optical trap.

References

[1] Cross, R. and Scholey, J. (1999) Nat. Cell Biol. 1, E119–E121.
[2] Rice, S. et al. (1999) Nature 402, 778–784.
[3] Case, R.B., Rice, S., Hart, C.L., Ly, B. and Vale, R.D. (2000) Curr. Biol. 10, 157–160.
[4] Hopkins, S.C., Vale, R.D. and Kuntz, I.D. (2000) Biochemistry 39, 2805–2814.
[5] Howard, J., Hudspeth, A.J. and Vale, R.D. (1989) Nature 342, 154–158.
[6] Svoboda, K. and Block, S.M. (1994) Cell 77, 773–784.
[7] Visscher, K., Schnitzer, M.J. and Block, S.M. (1999) Nature 400, 184–189.
[8] Schnitzer, M.J. and Block, S.M. (1997) Nature 388, 386–390.
[9] Hua, W., Young, E.C., Fleming, M.L. and Gelles, J. (1997) Nature 388, 390–393.
[10] Coy, D.L., Wagenbach, M. and Howard, J. (1999) J. Biol. Chem. 274, 3667–3671.
[11] Vale, R.D., Reese, T.S. and Sheetz, M.P. (1985) Cell 42, 39–50.
[12] Sharp, D.J., Rogers, G.C. and Scholey, J.M. (2000) Biochim. Biophys. Acta 1496, 128–141.
[13] Lockhart, A. and Cross, R.A. (1994) EMBO J. 13, 751–757.
[14] Crevel, I., Carter, N., Schliwa, M. and Cross, R. (1999) EMBO J. 18, 5863–5872.
[15] Hodge, T.P., Cross, R. and Kendrick-Jones, J. (1992) J. Cell Biol. 118, 1085–1095.
[16] Cross, R.A., Geeves, M.A. and Kendrick-Jones, J. (1991) EMBO J. 10, 747–756.
[17] Cross, R.A., Crevel, I., Carter, N.J., Alonso, M.C., Hirose, K. and Amos, L.A. (2000) Philos. Trans. R. Soc. Lond. B 355, 459–464.
[18] Stewart, R.J., Thaler, J.P. and Goldstein, L.S. (1993) Proc. Natl. Acad. Sci. USA 90, 5209–5213.
[19] Chandra, R., Salmon, E.D., Erickson, H.P., Lockhart, A. and Endow, S.A. (1993) J. Biol. Chem. 268, 9005–9013.
[20] Grummt, M., Woehlke, G., Henningsen, U., Fuchs, S., Schleicher, M. and Schliwa, M. (1998) EMBO J. 17, 5536–5542.